symmetry

MDPI

Article

Distortion-Corrected Integral Imaging 3D Display System Based on Lens Array Holographic Optical Element

Jun-Hua Li [1], Han-Le Zhang [2,*], Qing-Lin Ji [1] and Wu-Xiang Zhao [1]

[1] College of Electronics and Information Engineering, Sichuan University, Chengdu 610065, China; sanlang6969@163.com (J.-H.L.); jiqinglin@stu.scu.edu.cn (Q.-L.J.); zhaowuxiang@scu.edu.cn (W.-X.Z.)
[2] School of Instrumentation and Optoelectronics Engineering, Beihang University, Beijing 100191, China
* Correspondence: hanlezhang@buaa.edu.cn

Abstract: We propose a distortion-corrected integral imaging (II) 3D display system based on lens array holographic optical element (LAHOE). The LAHOE is used as a projection screen. The projection beam of the LAHOE is parallel light. Hence, the projection system consists of a spatial light modulator, a reverse projection lens, a relay optical element, and a telecentric lens. The acquired 3D data and the reconstructed 3D image of II are symmetrically related to each other. Therefore, there is lens distortion in the projection system. To avoid affecting the viewing experience of the viewers, the elemental image array (EIA) is projected obliquely on the LAHOE, causing the lateral distortion of the EIA. There is a position deviation in the projection system, so the projected EIA has geometric deformation. Due to the distortion of the EIA, it is difficult to precisely align the projected EIA and LAHOE, which results in serious flip of the reconstructed 3D images. The distortion of the EIA affects the asymmetry of the 3D image reconstruction. Lens distortion can be solved by the distortion compensation method. Lateral and the geometric deformation can be solved by the perspective transformations in computer graphics. After correction, the undistorted EIA is projected, and the projected EIA on the LAHOE has little distortion. In the process of 3D image reconstruction, the causes of asymmetry affecting 3D image reconstruction are analyzed, and the issues that generate these asymmetric factors are addressed. Experimental results indicate that a better 3D display effect is achieved.

Keywords: 3D display; integral imaging; lens-array holographic optical element; elemental imaging array

Citation: Li, J.-H.; Zhang, H.-L.; Ji, Q.-L.; Zhao, W.-X. Distortion-Corrected Integral Imaging 3D Display System Based on Lens Array Holographic Optical Element. *Symmetry* **2022**, *14*, 1481. https://doi.org/10.3390/sym14071481

Academic Editors: Xiaowei Li, Shu-Feng Lin, Yan Xing and Alexey V. Lukoyanov

Received: 21 May 2022
Accepted: 7 July 2022
Published: 20 July 2022

1. Introduction

Recently, augmented reality has received wide attention, and it can overlay virtual images into real scenes [1]. To achieve augmented reality display, see-through optical elements are used as image synthesizing elements [2]. For decades, augmented reality has been the 2D display. With the development of the autostereoscopic 3D display, the see-through autostereoscopic 3D display will be the core of the next generation of augmented reality.

The autostereoscopic 3D display includes holographic display [3,4], multi-view display [5,6], integrated imaging display [7,8], and other display technologies. The integral imaging 3D display is considered to be one of the most promising 3D displays. It has the advantages of a continuous viewing point, full parallax, full-color display, and ignoring fatigue [9,10]. Therefore, many researchers combine II 3D display technology with augmented reality technology and propose an augmented reality 3D display system by using a LAHOE as the image synthesizing element. For example, Seoul National University has developed a full-color LAHOE for 3D optical see-through augmented reality [11], proposed a without a pseudoscopic problem 3D display using a phase-conjugated reconstruction of LAHOE [12], released a 2D/3D switchable display system based on LAHOE [13], proposed an enhanced resolution 3D see-through display system [14], and developed an enhanced viewing angle II 3D display [15]. The Tokyo Institute of Technology has developed a 3D

touchable holographic light-field display system [16]. Our group has developed a tabletop augmented reality 3D display system based on II [17] and released a dual-view-zone tabletop 3D display system based on integral imaging by using a multiplexed holographic optical element [18].

The acquired 3D data and the reconstructed 3D image of II are symmetrically related to each other. The LAHOEs of the above system are being used as a projection screen; the projection beam of the LAHOE is parallel light. So, the projection system consists of a spatial light modulator, a reverse projection lens, a relay optical element, and a telecentric lens. The telecentric lens and relay optics are used to collimate and expand the projection beam. Finally, the collimated light with EIA is projected on the LAHOE with an incident angle of θ. The structure of the projection system is shown in Figure 1. Because the projection system is not correct, the projection beam changes in the direction of the curvature of the projection lens, which is represented by the radial ratio distortion. It causes the image point to be shifted along the radial direction, and the larger the deformation is from the center point; this is the radial distortion of the projection system. In the assembly process of the projection system, the optical axis of the lens that comprises the projection system is not collinear. The present optical system is affected by eccentricity, leading to distortion of the image; this is the tangential distortion of the projection system. The distortion of the prism is mainly due to the manufacturing error of the projector CCD imaging matrix and the manufacturing error of the projection system objective. So, there is lens distortion in the projection system.

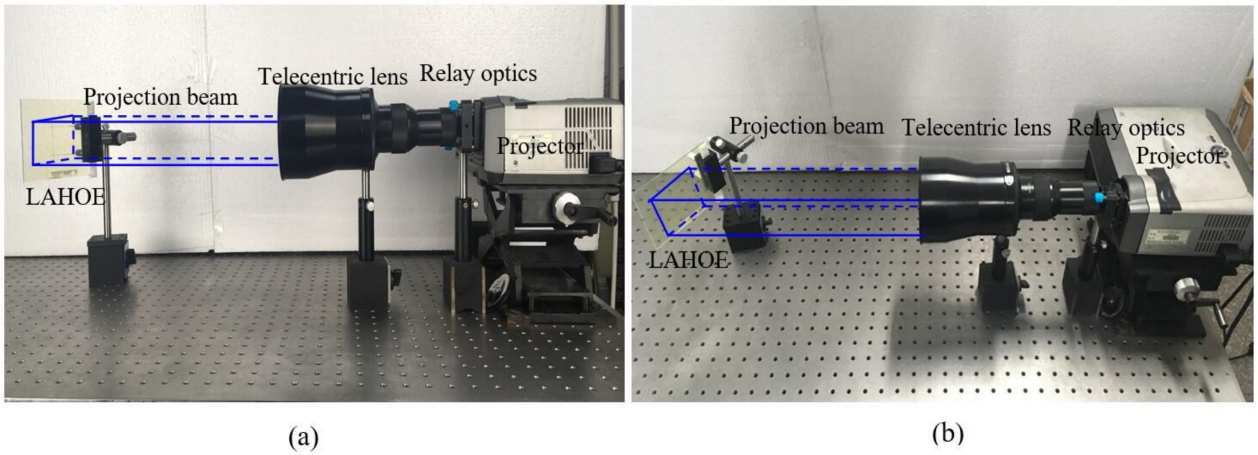

Figure 1. The structure of the projection system, (**a**) the section diagram of the projection system, and (**b**) the top viewport of the projection system.

These LAHOEs of the above systems use the optical principle of off-axis imaging, which requires that the projection beam be projected at a certain angle θ. As a result, the lateral distortion of the EIA occurs when the projection beam is projected onto the LAHOE, as shown in Figure 2a. Because of the position shift of the projector, the EIA has geometric deformation, as shown in Figure 2b. In the reconstruction process, an obliquely incident display beam leads to the different pixel densities in horizontal and vertical directions, which causes the difference in the angular resolution of 3D images in horizontal and the vertical directions. Because of elemental image array (EIA) distortions, it is difficult to accurately align the EIA with the LAHOE. Serious flip exists in the reconstructed 3D images, and it is difficult to build a large 3D display system. The distortion of the EIA affects the asymmetry of the 3D image reconstruction.

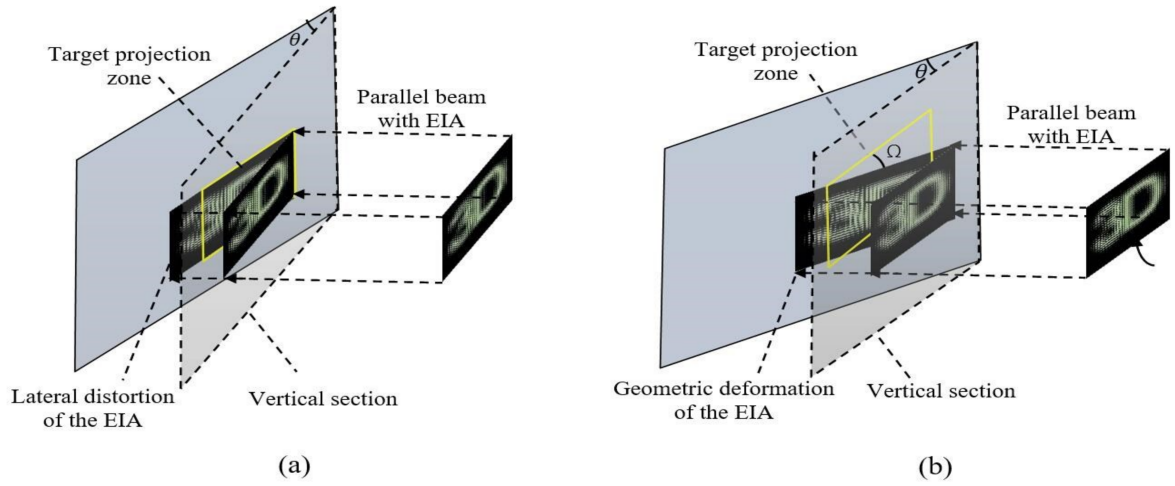

Figure 2. (**a**) Lateral distortion of the EIA, (**b**) geometric deformation of the EIA.

To solve the problem of the lateral distortion of the EIA, the Seoul National University has developed an on-axis LAHOE for a see-through integral imaging 3D display system [19]; this system effectively solves the issue of the lateral distortion of the EIA but it does not solve the geometric of the EIA. Moreover, the diffraction beam and the reflected beam of the LAHOE cannot be separated. Therefore, the diffraction beams and the reflected beam of the LAHOE overlap each other, so the reconstructed 3D image is not clear, and it has serious crosstalk problems. The Tokyo Institute of Technology has developed a rapid calibration of a projection-type holographic light-field display system using hierarchically unconverted binary sinusoidal patterns [20]. This method could rapidly calibrate the projection-type II 3D display system and solves the problem of the lateral distortion and the geometric deformation of the EIA.

To precisely align EIA and LAHOE, our group precorrected the lens distortion of the projection system, the distortion compensation method can be used to compensate for the lens distortion, and the EIA of before the project, based on the perspective transformation in computer graphics, can be used to resolve the lateral distortion and geometric deformation. In the process of 3D image reconstruction, the causes of asymmetry affecting 3D image reconstruction are analyzed and the issues that generate these asymmetric factors are addressed. As a result, the projected EIA has a uniform pixel density in the horizontal and vertical directions, and the precise alignment between EIA and LAHOE is realized.

2. System Configuration

To realize the precise couple between EIA and LAHOE, the projection beam in the reconstruction process makes the uniform pixel density in the horizontal and vertical directions. The distortion is caused by the projection lens. The lateral distortion and geometric deformation of the EIA are caused by the projection system. The causes of asymmetry affecting 3D image reconstruction are analyzed. Thus, an examination of the projection lens is performed first, and then lateral distortion and geometric deformation of the EIA in the projection system are analyzed.

2.1. Lens Distortion of the Projection System

The projection system consists of a spatial light modulator, a reverse projection lens, a relay optical element, and a telecentric lens. As shown in Figure 1. The projection system is not corrected. Therefore, there has lens distortion in the projection system. The lens distortion of the projection system includes radial distortion, tangential distortion, and thin prism distortion. The lens distortion cannot be solved by the perspective transformation. Assuming the coordinates of the projective point without lens distortion are (x_p, y_q). The coordinates of the projection points with lens distortion are (x_u, y_v). The projection beam changes in the direction of the curvature of the projection lens, which is represented by

the radial proportion distortion. It causes the image point to be shifted along the radial direction, and farther away from the center point. The mathematical model of the radial distortion can be expressed as:

$$\begin{cases} \delta x_r = k_1 x_u \left(x_u^2 + y_v^2\right) + O[(x_u, y_v)^5] \\ \delta y_r = k_2 y_u (x_u^2 + y_v^2) + O[(x_u, y_v)^5] \end{cases} \tag{1}$$

δx_r, δy_r are the number of distortions in the horizontal and vertical direction caused by radial distortion and k_1, k_2 are the radial distortion coefficients.

In the assembly process of the projection system, the optical axis of the lens that consists of the projection system is not collinear. The actual optical system is affected by eccentricity, resulting in the distortion of the image. The mathematical model of tangential distortion can be expressed as:

$$\begin{cases} \delta x_d = p_1 x_u (3x_u^2 + y_v^2) + 2p_2 x_u y_v + O[(x_u, y_v)^4] \\ \delta y_d = 2p_1 x_u y_v + p_2 x_u (x_u^2 + 3y_v^2) + O[(x_u, y_v)^4] \end{cases} \tag{2}$$

δx_d, δy_d are the number of distortions in the horizontal and vertical direction caused by tangential distortion and p_1, p_2 are the tangential distortion coefficients.

The thin prism distortion is mainly caused by the CCD imaging array manufacturing error of the projector and the lens manufacturing error of the projection system. The mathematical model can be expressed as:

$$\begin{cases} \delta x_p = s_1 (x_u^2 + y_v^2) + O[(x_u, y_v)^4] \\ \delta y_p = s_2 (x_u^2 + y_v^2) + O[(x_u, y_v)^4] \end{cases} \tag{3}$$

δx_p, δy_p are the number of distortions in the horizontal and vertical direction caused by thin prism distortion and s_1, s_2 are the thin prism distortion coefficients. Therefore, without lens distortion imaging, the point coordinates are the sum of the with lens distortion imaging point coordinates and the number of the distortions of the imaging point, which can be expressed as:

$$\begin{cases} x_p = x_u + \delta x_r + \delta x_d + \delta x_p \\ y_q = y_v + \delta y_r + \delta y_d + \delta y_p \end{cases} \tag{4}$$

k_1, k_2, p_1, p_2, s_1, s_2 are the lens distortion coefficients and Equation (4) can be expressed as:

$$CP = D - E \tag{5}$$

Of these:

$$C = \begin{bmatrix} x_u(x_u^2 + y_v^2) & 0 & 3x_u^2 + y_v^2 & 2x_u y_v & x_u^2 + y_v^2 & 0 \\ 0 & y_v(x_u^2 + y_v^2) & 2x_u y_v & x_u^2 + y_v^2 & 0 & x_u^2 + y_v^2 \end{bmatrix} \tag{6}$$

$$P = \begin{bmatrix} k_1 & k_2 & p_1 & p_2 & s_1 & s_2 \end{bmatrix}^T \tag{7}$$

D is the coordinate matrix of the projective point without lens distortion and E is the coordinate matrix of the projection points with lens distortion. The six coefficients of the lens distortion can be solved by three pairs of target values and actual values of the measured pixels. To obtain the lens distortion parameters, we selected the central position of the projection zone and obtain three pairs of the distortion values and the actual values of the closest point in the center of the projection zone. To improve the calculation precision, the distortion coefficient vector P was obtained by the least square method. Then, the height mapping relation between the coordinate matrix of the projective point without lens distortion and the coordinate matrix of the projection points with lens distortion was obtained by Equation (5):

$$D = CP + E \tag{8}$$

Thus, the projection zone without lens distortion was obtained.

2.2. The Lateral Distortion and Geometric Deformation of the EIA

The lens distortion of the projection system has been solved. However, the lateral distortion and geometric deformation of the EIA remains to be resolved. As shown in Figure 3, we must correct the distorted EIA image and project the non-deformed EIA into the target projection zone. The distortion of the EIA is corrected by the method of pre-correction the distortion of perspective transformation in computer graphics.

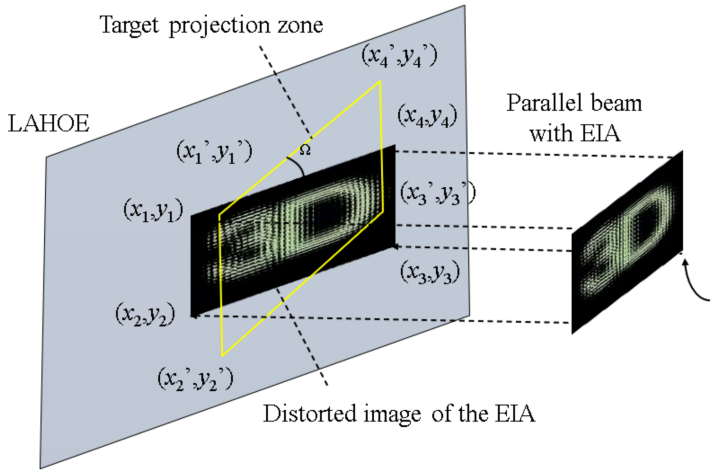

Figure 3. Correction principle between the distorted image and the target projection zone.

In computer graphics, perspective transformation is defined as a mapping from one plan to another. Perspective transformation can extract the translation and rotation matrix between two images from the homography matrix, and it is rendered based on the correct mapping relation, which satisfies the linear relationship. Assume that point Q (x_p, y_q, z) is an image point projected onto the LAHOE without lens distortion by the projection system. P (x, y) is a target projection zone image point of the Q after the perspective transformation. The relationship between them can be expressed as:

$$\begin{bmatrix} x \\ y \\ 1 \end{bmatrix} = A \begin{bmatrix} R & t \end{bmatrix} \begin{bmatrix} x_p \\ y_q \\ z \\ 1 \end{bmatrix} \tag{9}$$

$\boldsymbol{A}$ is the internal reference matrix of the projection system, which includes the image main point (u_0, v_0), the focal length f_u in the x-direction, and the focal length f_v in the y-direction of the image coordinates. $\boldsymbol{R}$ and $\boldsymbol{t}$ are the external reference matrix of the projection system. $\boldsymbol{R}$ consists of three rotation angles, α is the light axis pitching angle, β is the light yaw angle, and φ is the rotation angle of the light. The translation matrix $\boldsymbol{t}$ consists of t_x, t_y, and t_z translation vectors in three directions. Therefore, the lateral distortion can be solved by the translation matrix $\boldsymbol{t}$ and the geometric deformation can be solved by the rotation matrix $\boldsymbol{R}$.

The homography matrix between the real imaging zone and the target projection imaging zone can be expressed as:

$$\begin{bmatrix} x \\ y \\ 1 \end{bmatrix} = \begin{bmatrix} a & b & e \\ c & d & f \\ u & v & g \end{bmatrix} \begin{bmatrix} x_p \\ y_q \\ 1 \end{bmatrix} \tag{10}$$

Because it is a transformation in a two-dimensional plane, the coordinates of the z-axis direction are removed. From Equation (10) the following two Equations can be obtained through:

$$\begin{bmatrix} -x_p & -y_q & -1 & 0 & 0 & 0 & x_p x & y_q x & x \\ 0 & 0 & 0 & -x_p & -y_q & -1 & x_p y & y_q y & y \end{bmatrix} h = 0 \tag{11}$$

$$h = \begin{bmatrix} a & b & e & c & d & f & u & v & g \end{bmatrix} \tag{12}$$

In normalized processing, where g = 1, eight variables need to be calculated. So, the matrix can be calculated by four pairs of matching points. Assume, (x_1, y_1), (x_2, y_2), (x_3, y_3), and (x_4, y_4) are four orientations in the original coordinate system of the distorted image of EIA without lens distortion, $(x_{1'}, y_{1'})$, $(x_{2'}, y_{2'})$, $(x_{3'}, y_{3'})$, and $(x_{4'}, y_{4'})$ are the corresponding point of target projection coordinate after projection transformation of the EIA. The relationship between them can be expressed as:

$$\begin{bmatrix} x' \\ y' \end{bmatrix} = \frac{\begin{bmatrix} a & b \\ c & d \end{bmatrix} \begin{bmatrix} x \\ y \end{bmatrix} + \begin{bmatrix} e \\ f \end{bmatrix}}{1 + \begin{bmatrix} u & v \end{bmatrix} \begin{bmatrix} x \\ y \end{bmatrix}} \tag{13}$$

a, b, c, d, e, f, u, and v are the correction coefficients of the projection system. When the correction coefficients of the projection system are obtained, the distortion precorrection of the EIA can be determined, and the pixel mapping relationship between the mapping target projection zone and the original projection zone of the distorted image of EIA can be determined.

2.3. Correction of the Projection Zone

The correction process of the target projection zone is shown in Figure 3. Before the correction, the checkerboard cannot overlap the target projection zone completely, because the checkerboard has lateral distortion, geometric deformation, and lens distortion, as shown in Figure 3, and Figure 4a shows that the projection system has lens distortion, lateral distortion, and geometric deformation. Equation (8) is used to correct the lens distortion. Then Equation (13) is used to correct the lateral distortion and geometric deformation. The corrected projection system has an extremely low distortion. The corrected checkerboard matches the target projection zone exactly, as shown in Figure 4b.

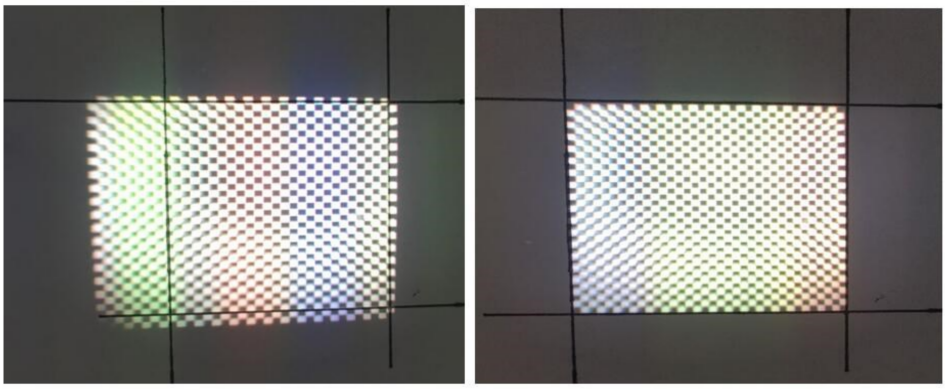

(a) (b)

Figure 4. Checkerboard correction process, (**a**) before correction with distortion, (**b**) after correction without distortion.

3. Experiment and Results

The fabrication principle of the LAHOE is shown in Figure 5. The fabrication of the LAHOE is the typical reflective holographic optical element. The interference pattern formed by an oblique plane wave reference beam and the spherical wave array, containing properties of the conventional lens array, is recorded into the holographic material in front

of the lens array. In the experiment, a green solid-state laser with a power of 2000 mW was used as the light source, and the green-sensitive photopolymer material was used to fabricate the LAHOE. The thickness of the photopolymers is 15 μm; the refractive index of the polymer materials is 1.47, and the resolution of the polymer materials is 12,000 line/mm. The specific parameters of the optical devices are shown in Table 1. An 80 mm × 90 mm large size LAHOE was fabricated, and the wavefronts of the lens array were reconstructed through white light, as shown in Figure 6. The pitch of the lens elemental is 1 mm and the focal length is 3.3 mm. The diffraction efficiency of LAHOE is 84%.

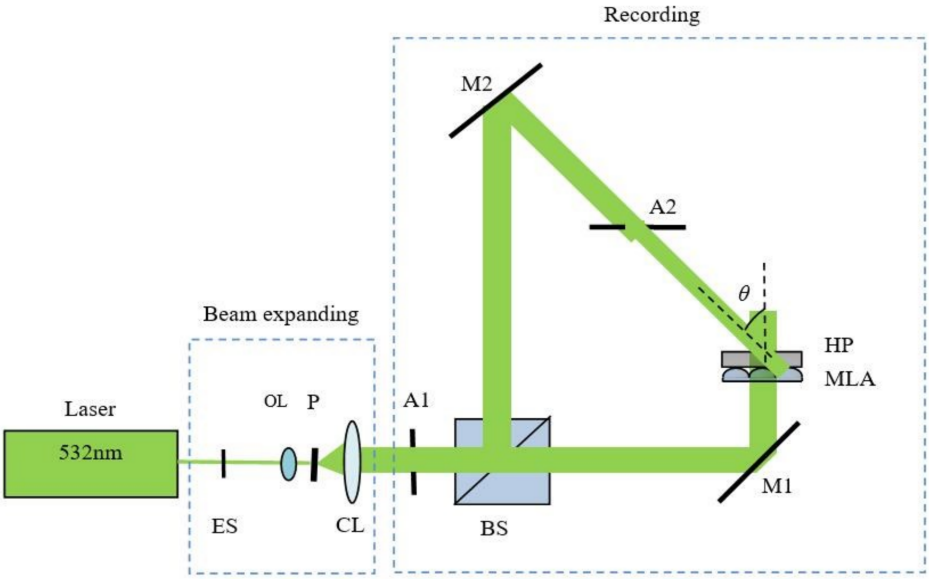

Figure 5. Schematic diagrams for fabrication of the LAHOE. ES, electronic shutter; OL, objective lens; P, pinhole; CL, collimating lens; A, aperture; BS, beam splitter; M, mirror; HP, holographic plate; MLA, micro-lens array.

Table 1. Specific parameters of the optical devices.

Components	Parameters	Values
Solid-state laser	Power	2000 mW
	Wavelength	532 nm
Green-sensitive photopolymer material	Thickness	15 ± 1 μm
	Resolution	12,000 line/mm
	Sensitive wavelength	532 nm
	Refractive index modulation	>0.02
	Refractive index	1.47
Lens-array	Pitch	1 mm
	Focal length	3.3 mm
Beam splitter	Coupling ratio	1:1

The experimental setup for the reconstruction of the 3D image is shown in Figure 7. The magnification of the telecentric lens is limited, only a 50 mm × 38 mm rectangular parallel beam can be projected. Therefore, we chose the 35 mm × 35 mm region as the target projection zone on the large-size LAHOE. The telecentric lens and the relay optics serve to collimate the beam projected by the projector. The collimated projection beam with elemental image array was projected on the LAHOE with the incident angle of 45°. When the projection beam reaches the LAHOE, some of the beam produces diffracted light waves and reconstructs the 3D image, and one portion of the projection beam is reflected,

and another portion of the projection beam crosses the LAHOE. The camera was used to obtain the 3D images of the diffracted beam reconstruction. The EIA was generated by the computer, as shown in Figure 8. The EIA consists of 35 × 35 image elements, it contains "3" and "D", in which the position of "3" is +6 mm and the "D" position is −6mm.

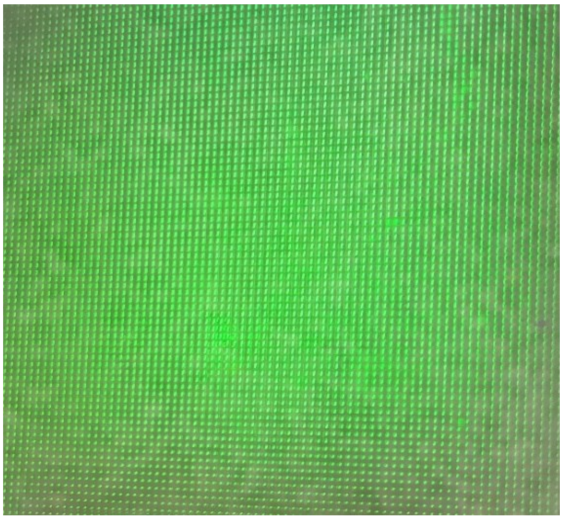

Figure 6. Reconstruction of the lens array using the LAHOE with Bragg matched light.

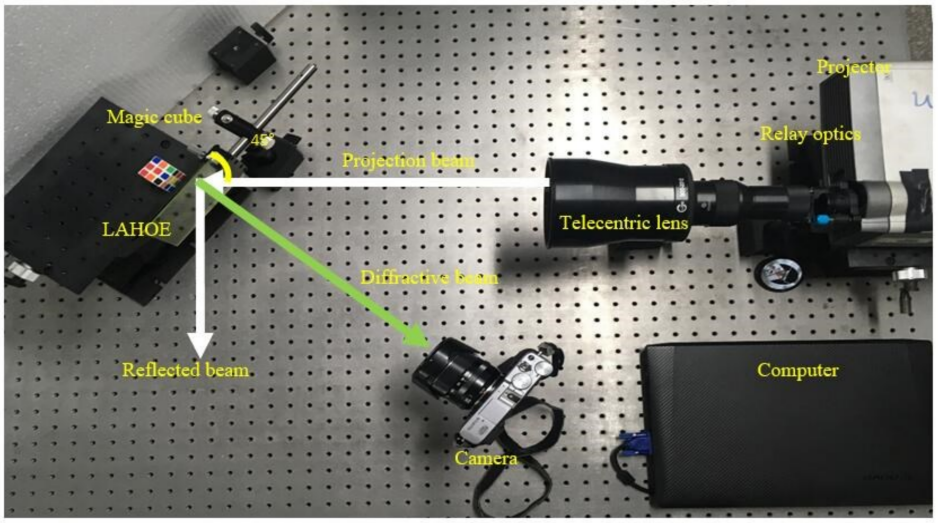

Figure 7. Experimental setup of reconstruction 3D images.

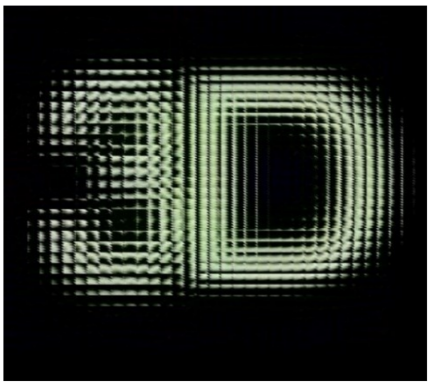

Figure 8. Elemental images for reconstruction of 3D images.

After correction of distortion of EIA, the EIA, and LAHOE realize precise coupling. In the process of 3D image reconstruction, the pixel density of the projection beam in the horizontal and vertical direction is uniform, as shown in Figure 9a,b. In the reconstruction process, the projection beam was used to irradiate LAHOE. The LAHOE has the optical properties of a micro-lens array when Bragg conditions are satisfied. The EIA information carried in the reference light wave was modulated by the LAHOE to reconstruct the 3D image. We obtained four pictures from the left, right, top, and bottom four viewpoints. The distortion of EIA was eliminated. We can see the horizontal parallax of the virtual "3D" from the left and right images and the vertical parallax of the virtual "3D" from the top and bottom images. The reconstructed 3D images have obvious horizontal and vertical parallaxes. Visualization 1 clearly shows the horizontal and vertical parallaxes between the "3", "D", and the real-world scene. Reconstructed 3D images exhibit uniform pixel density in horizontal and vertical directions.

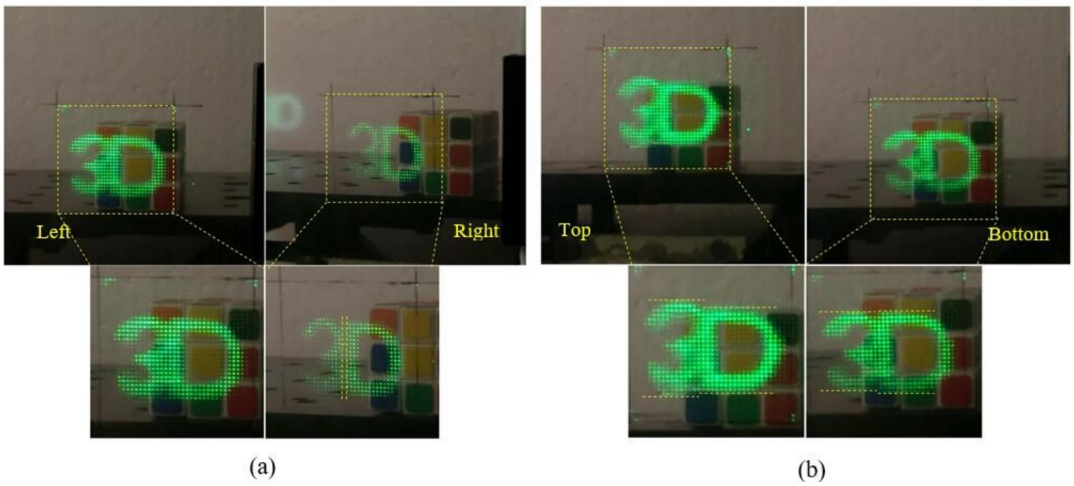

Figure 9. Reconstructed 3D images of distortion correction (see **Visualization 1**), (**a**) horizontal viewing parallax, and (**b**) vertical viewing parallax.

The 3D images reconstructed by the EIA without any correction are shown in Figure 10. The EIA exhibits lateral distortion, geometric deformation, and lens distortion, such that the EIA cannot be accurately coupled to the LAHOE. Consequently, it has different densities of pixel in horizontal and vertical directions, which causes the difference in the angular resolution of 3D images in horizontal and vertical directions. Reconstructed 3D images have serious crosstalk, weak definition, and poor image quality, and the stereoscopic sense of reconstructed 3D image is not evident. We obtained four pictures from the left, right, top, and bottom four viewpoints. We can see the horizontal parallax of the virtual "3D" from the left and right images, and the vertical parallax of the virtual "3D" from the top and bottom images, but the 3D images have serious crosstalk and weak stereoscopics. The pixel densities are different in the horizontal and the vertical directions, and the resolution of the reconstructed 3D images is different in the horizontal and vertical directions. Visualization 2 shows the horizontal and vertical parallaxes between the "3", "D", and the real-world scene, but the 3D images have serious crosstalk.

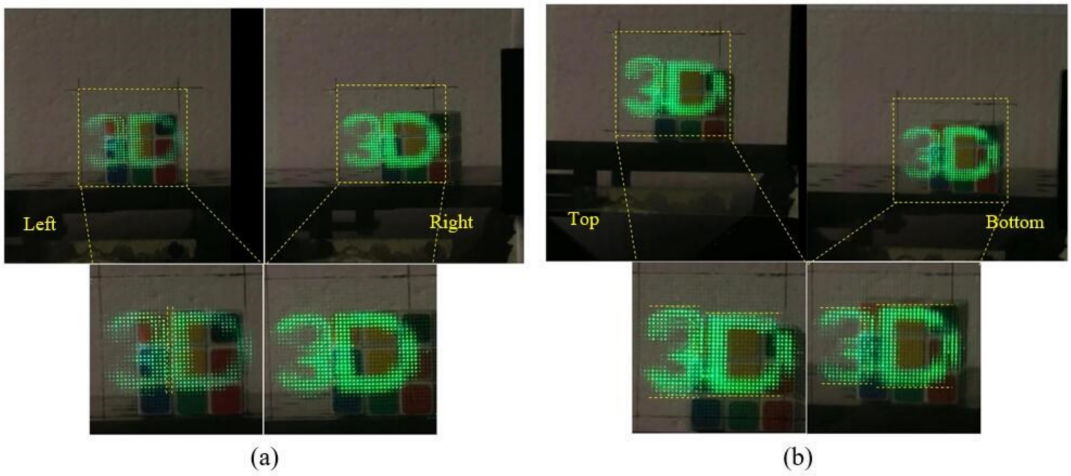

Figure 10. Reconstructed 3D images of distortion without correction (See **Visualization 2**), (**a**) horizontal viewing parallax, and (**b**) vertical viewing parallax.

4. Conclusions

In conclusion, we propose a distortion-corrected projection-type see-through II 3D display system based on LAHOE. Based on the principle of the projection lens distortion and the projection system in computer graphics, the problem of lens distortion, lateral distortion, and geometric deformation of the EIA is eliminated. In the process of 3D image reconstruction, the causes of asymmetry affecting 3D image reconstruction are analyzed, and the issues that generate these asymmetric factors are addressed. The EIA is closely coupled with the LAHOE, and the 3D images with high image quality and significant sense of stereoscopic are reconstructed. The projection beam in the reconstruction process makes the uniform pixel density in horizontal and vertical direction. The resolution of the reconstructed 3D images is uniform in horizontal and vertical direction. In the reconstruction of the small-size see-through II 3D display, the mismatch between the EIA and LAHOE is not obvious. However, the mismatch between EIA and LAHOE is highlighted in large-size see-through II 3D display. The system provides a solution for the reconstruction of the large-size see-through II 3D display.

Author Contributions: Conceptualization, J.-H.L., and H.-L.Z.; methodology, J.-H.L.and H.-L.Z.; software, J.-H.L., H.-L.Z., Q.-L.J. and W.-X.Z.; data curation and writing-original draft preparation, J.-H.L. and H.-L.Z.; writing—review and editing, Q.-L.J. and W.-X.Z.; All authors have read and agreed to the published version of the manuscript.

Funding: This research is supported by National Natural Science Foundation of China under grant No. 62105016, the China Postdoctoral Science Foundation under grant No. 2021M690287, and the Applied Basic Research Program of Sichuan province under grant No. 2021YJ0094.

Institutional Review Board Statement: Not applicable.

Informed Consent Statement: Not applicable.

Data Availability Statement: Data is contained within the article.

Conflicts of Interest: The authors declare no conflict of interest.

References

1. Azuma, R.; Baillot, Y.; Behringer, R.; Feiner, S.; Julier, S.; MacIntyre, B. Recent advances in augmented reality. *IEEE Comput. Graph. Appl.* **2001**, *21*, 34–47. [CrossRef]
2. Kiyokawa, K.; Billinghurst, M.; Campbell, B.; Woods, E. An occlusion capable optical see-through head mount display for supporting co-located collaboration. In Proceedings of the Second IEEE and ACM International Symposium on Mixed and Augmented Reality, Tokyo, Japan, 10 October 2003.
3. Zhao, Y.; Cao, L.; Zhang, H.; Kong, D.; Jin, G. Accurate calculation of computer-generated holograms using angular-spectrum layer-oriented method. *Opt. Express* **2015**, *23*, 25440–25449. [CrossRef] [PubMed]

4. Zhang, H.; Zhao, Y.; Cao, L.; Jin, G. Fully computed holographic stereogram-based algorithm for computer-generated holograms with accurate depth cues. *Opt. Express* **2015**, *23*, 3901–3913. [CrossRef]
5. Lv, G.-J.; Wang, J.; Zhao, W.-X.; Wang, Q.-H. Three-dimensional display based on dual parallax barriers with uniform resolution. *Appl. Opt.* **2013**, *52*, 6011–6015. [CrossRef]
6. Zhao, R.L.; Zhao, W.X.; Wang, Q.H.; Li, D.H.; Wang, A.H.; Xin, Y.X. Research on stereo viewing zone in autostereoscopic display based on parallax barrier. *Acta. Photonica Sin.* **2008**, *121*, 96–98.
7. Zhang, H.-L.; Deng, H.; Yu, W.-T.; Wang, Q.-H.; He, M.-Y.; Li, D.-H. Tabletop augmented reality 3D display system based on integral imaging. *J. Opt. Soc. Am. B* **2017**, *34*, B16–B21. [CrossRef]
8. Fan, Z.-B.; Qiu, H.-Y.; Zhang, H.-L.; Pang, X.-N.; Zhou, L.-D.; Liu, L.; Ren, H.; Wang, Q.-H.; Dong, J.-W. A broadband achromatic metalens array for integral imaging in the visible. *Light Sci. Appl.* **2019**, *8*, 67. [CrossRef] [PubMed]
9. Javidi, B.; Carnicer, A.; Arai, J.; Fujii, T.; Hua, H.; Liao, H.; Martínez-Corral, M.; Pla, F.; Stern, A.; Waller, L.; et al. Roadmap on 3D integral imaging: Sensing, processing, and display. *Opt. Express* **2020**, *28*, 32266–32293. [CrossRef]
10. Wang, X.; Hua, H. Depth-enhanced head-mounted light field display based on integral imaging. *Opt. Lett.* **2021**, *46*, 985–988. [CrossRef] [PubMed]
11. Hong, K.; Yeom, J.; Jang, C.; Hong, J.; Lee, B. Full-color lens-array holographic optical element for three-dimensional optical see-through augmented reality. *Opt. Lett.* **2014**, *39*, 127–130. [CrossRef] [PubMed]
12. Yeom, J.; Hong, K.; Jeong, Y.; Jang, C.; Lee, B. Solution for pseudoscopic problem in integral imaging using phase-conjugated reconstruction of lens-array holographic optical elements. *Opt. Express.* **2014**, *22*, 13659–13670. [CrossRef] [PubMed]
13. Yeom, J.; Jeong, J.; Jang, C.; Li, G.; Hong, K.; Lee, B. Three-dimensional/two-dimensional convertible projection screen using see-through integral imaging based on holographic optical element. *Appl. Opt.* **2015**, *54*, 8856–8862. [CrossRef] [PubMed]
14. Jang, C.; Hong, K.; Yeom, J.; Lee, B. Three-dimensional see-through display using resolution enhanced lens-array holographic optical element. In Proceedings of the 75th JSAP Autumn Meeting, Sapporo, Japan, 17–20 September 2014.
15. Lee, S.; Jang, C.; Cho, J.; Yeom, J.; Jeong, J.; Lee, B. Viewing angle enhancement of an integral imaging display using Bragg mismatched reconstruction of holographic optical elements. *Appl. Opt.* **2016**, *55*, A95–A103. [CrossRef] [PubMed]
16. Yamaguchi, M.; Higashida, R. 3D touchable holographic light-field display. *Appl. Opt.* **2016**, *55*, A178–A183. [CrossRef] [PubMed]
17. Zhang, H.-L.; Deng, H.; Yu, L.J.-J.; He, M.-Y..; Li, D.-H.; Wang, Q.-H. Integral imaging-based 2D/3D convertible display system by using holographic optical element and polymer dispersed liquid crystal. *Opt. Lett.* **2019**, *44*, 387–390. [CrossRef] [PubMed]
18. He, M.; Zhang, H.; Deng, H.; Li, D.; Wang, Q. Dual-view-zone table-top 3D display system based on integral imaging. *Appl. Opt.* **2018**, *57*, 952–958. [CrossRef] [PubMed]
19. Jang, C.; Lee, C.-K.; Jeong, J.-J.; Lee, S.; Yeom, J.; Hong, K.; Lee, B. Recent progress in see-through three-dimensional displays using holographic optical elements. *Appl. Opt.* **2016**, *55*, A71–A85. [CrossRef] [PubMed]
20. Nakamura, F.; Yamaguchi, M. Rapid calibration of a projection-type holographic light-field display system using hierarchically unconverted binary sinusoidal patterns. *Appl. Opt.* **2017**, *56*, 9520–9525. [CrossRef] [PubMed]